



Mechanism of Organic Matter Accumulation in Black Shales of the Yuertusi Formation in the Tarim Basin: Insights From Paleoenvironmental Variation During the Early Cambrian

OPEN ACCESS

Edited by:

Kun Zhang,
Southwest Petroleum University,
China

Reviewed by:

Ling Tang,
CNOOC Research Institute Ltd., China
Wei Li,
University of Nottingham,
United Kingdom
Zhipeng Huo,
Northeastern University at
Qinhuangdao, China

***Correspondence:**

Weibing Shen
swb560316@126.com

†Present address:

Weibing Shen,
Institute of Geology, Chinese
Academy of Geological Sciences,
Beijing, China

Specialty section:

This article was submitted to
Geochemistry,
a section of the journal
Frontiers in Earth Science

Received: 20 February 2022

Accepted: 07 March 2022

Published: 30 March 2022

Citation:

Wang Y, Chen J, Shen W and Li M
(2022) Mechanism of Organic Matter
Accumulation in Black Shales of the
Yuertusi Formation in the Tarim Basin:
Insights From Paleoenvironmental
Variation During the Early Cambrian.
Front. Earth Sci. 10:879658.
doi: 10.3389/feart.2022.879658

Yangyang Wang¹, Jianfa Chen², Weibing Shen^{3*†} and Min Li⁴

¹National Institute of Natural Hazards, Ministry of Emergency Management of China, Beijing, China, ²State Key Laboratory of Petroleum Resources and Prospecting, China University of Petroleum, Beijing, China, ³MLR Key Laboratory of Isotope Geology, Institute of Geology, Chinese Academy of Geological Sciences, Beijing, China, ⁴National Research Center for Geoanalysis, Beijing, China

The paleoenvironment during the Early Cambrian is closely related to the accumulation mechanism of organic matter (OM) from the Lower Cambrian black shales. However, paleoenvironment remains a controversial issue. Here, we reported a lot of detailed data of sedimentary stratigraphy and geochemistry of the Lower Cambrian Yuertusi Formation in the Aksu area, Tarim Basin. The Yuertusi Formation from the Yutixi outcrop consists mainly of silicalite at the base, two sets of black shales, and crystalline dolostone. Based on the redox conditions traced by U/Th, V/Cr, Ni/Co, and V/Sc, the hydrothermal activity traced by Ce/Ce*, Cr/Zr, U/Th, Fe/Ti, and (Fe + Mn)/Ti ratios, as well as paleo-productivity traced by Ba, Cu, Rb/Sr, and other parameters, variations were observed in the depositional environments of the Yuertusi Formation: 1) the silicalite at the base was deposited under an euxinic condition and intense hydrothermal activity. Mo-U co-variation analysis revealed that the north margin of Tarim Basin belonged to the unrestricted marine during the Early Cambrian, 2) the lower black shales were deposited under an oxygen-poor condition and weak hydrothermal activity, and 3) the upper black shales were deposited under oxygen-poor, sub-oxic conditions and almost no hydrothermal activity. Although the hydrothermal activity improved paleo-productivity, the TOC values were low on the whole, which may be due to the intense hydrothermal activity that damaged the formation of source rocks. Comprehensive studies showed a gradually oxidizing environment and weakening paleo-productivity during the Yuertusi Formation deposited. The anoxic conditions were conducive to the preservation of OM, and the high-quality source rocks represented by the black shales of the Yuertusi Formation were formed, especially the first set of black shales. However, the enrichment of OM may be affected by the intense hydrothermal activity.

Keywords: black shales, Lower Cambrian, paleoenvironment, organic matter accumulation, Tarim Basin

1 INTRODUCTION

The black shales of the Lower Cambrian were widely distributed in the Tarim Basin (e.g., Lan et al., 2017; Li et al., 2018; Zhao et al., 2019; Kun Zhang et al., 2020; Zhang et al., 2022). With the expansion of hydrocarbon exploration to deep and ultra-deep formations in the Tarim Basin, ancient formations are increasingly attracting attention (Yu et al., 2009; Yao et al., 2014; Guo et al., 2017; Yao et al., 2017; Zhu et al., 2018), especially the deep Cambrian (Yun et al., 2014; Zhu et al., 2016; Zhu et al., 2019). The Cambrian source rock is considered to be the main contributor of the huge reserves of hydrocarbon (Jin et al., 2020; Chunyu Zhang et al., 2020). In particular, the black shales of the Lower Cambrian Yuertusi Formation have been confirmed as the highest quality marine source rocks discovered in China (Zhu et al., 2016).

In previous studies, the depositional environment of the Lower Cambrian source rocks in the study area had been studied by organic geochemistry, paleontology, petrology, and other methods (He et al., 2005; Dong et al., 2009; Liu et al., 2011; Chen et al., 2015; Hu et al., 2018). Due to the high degree of thermal evolution of source rocks of the Yuertusi Formation, some samples could not be effectively detected, resulting in strong multi-solution of data (Yao et al., 2011; Yang et al., 2017). More research works are required on the analysis of paleoenvironment. Jiang et al. (2007) believed that the Lower Cambrian black shales in the study area deposited in a complete anoxic environment. Yao et al. (2011) proposed that the oxygen-bearing surface water and the sub-oxidized/anoxic bottom water co-existed in Early Cambrian marine. The water body gushing from the bottom of paleo-marine was the main factor changing the sedimentary environment of the source rocks. Yang et al. (2017) deduced that the sedimentary environments of the two sets of black shales in the Yuertusi Formation were different. The first set was deposited in an anoxic (even euxinic) environment, while the second set was deposited in an anoxic environment and gradually transformed into a sub-oxidation environment. It can be seen that the depositional environment of the Lower Cambrian source rocks has been still controversial, especially the redox state of the Early Cambrian marine, which limited the study of the OM accumulation mechanism of source rocks in the target layers and brought difficulties to the evaluation of source rocks in the study area.

In this study, we generated an integrated geochemical dataset consisting of major and trace element data for black shales of the Lower Cambrian Yuertusi Formation in the Yutixi outcrop, combined with organic geochemical methods. The controlling effects of the paleo-marine redox state and hydrothermal activity on OM accumulation in the target layer were analyzed, which provided help for studying the OM accumulation mechanism of source rocks from the Lower Cambrian.

2 GEOLOGICAL SETTING AND SAMPLING SITE

2.1 Geological Setting

Tarim Basin is a multi-cycle superimposed basin composed of Paleozoic craton basin and Meso-Cenozoic foreland basin, which

experienced a long and complex process of formation, evolution, and transformation. It is one of the largest intracontinental basins containing hydrocarbon in the world and the only craton basin with high productivity of marine hydrocarbon in China (Jia and Wei, 2002; Liu et al., 2011; Pan et al., 2015; Zhu et al., 2016; Zhu et al., 2019). With relatively complex structural evolution, Tarim landmass experienced three structure–sedimentary cycles and deposited multiple sets of structural sequences (Dong et al., 2009; Liu et al., 2011; Wu et al., 2012; Zhu et al., 2016; Guo et al., 2017; Zhu et al., 2018) (**Figure 1**).

During the Early Cambrian, the Tarim Basin was situated at the southern margin of the nascent South Tianshan Ocean (Yu et al., 2009). The Aksu area in the northwestern margin of the Tarim Basin was deposited in a marine shelf sedimentary environment during the Early Cambrian. The Tarim Basin experienced post-rift subsidence and large-scale transgression, forming maximum sea flooding and transforming into epi-continental sea, and then deposited the Yuertusi Formation in the Early Paleozoic. In the extensional and weak extensional tectonic stress field, the Lower Cambrian Yuertusi Formation unconformably overlay the Qigebulake Formation dolomite as well as integrated contacts with the Xiaerbulake Formation, and widely distributed the layered silicalite and black shales (Zhou et al., 2014; Zhou et al., 2015). The deposition of the Yuertusi Formation was influenced by tectonic paleo-geomorphology, and the sedimentary lithologic characteristics varied greatly in different outcrops.

2.2 Sampling Site

The Yutixi outcrop is located in the southwest of the Aksu area, about 105 km away from Aksu City. The Yuertusi Formation at the Yutixi outcrop can be divided into six layers (**Figure 2**). The first layer is gray-black thin layered silicalite, interbedded with several layers of phosphorous block; the second layer is a set of black shales interbedded with phosphorous block; the third layer is gray-yellow silty dolomite with erosion structures, which had not been sampled; the fourth layer is a set of gray-green silty dolomite containing glauconite without sampling; the fifth layer is a set of black shales, interbedded with gray-black thin marlstone; and the sixth layer is gray thin micritic limestone, which is seriously weathered and has not been sampled. This study mainly focused on the first layer silicalite group (SG), the second layer black shales group (BG1), and the fifth layer black shales group (BG2), which can be regarded as a complete transgression–regression sedimentary cycle.

3 METHODS

Major elements in the samples were tested using an Axios mAX XRF spectrometer. The major elements in the samples were tested following the method described by Ryu et al. (2011). Whole rock powders were ground below 2 μm grain size.

Trace element concentrations were obtained using inductively coupled plasma mass spectrometry (ICP-MS). Trace element compositions of whole-rock samples were determined with analytical uncertainties generally better than 5% (2σ). The data qualities were monitored by the Chinese National standards (GSR-1, GSR-2, GSR-4, GSR-10, and GSR-16) for trace element

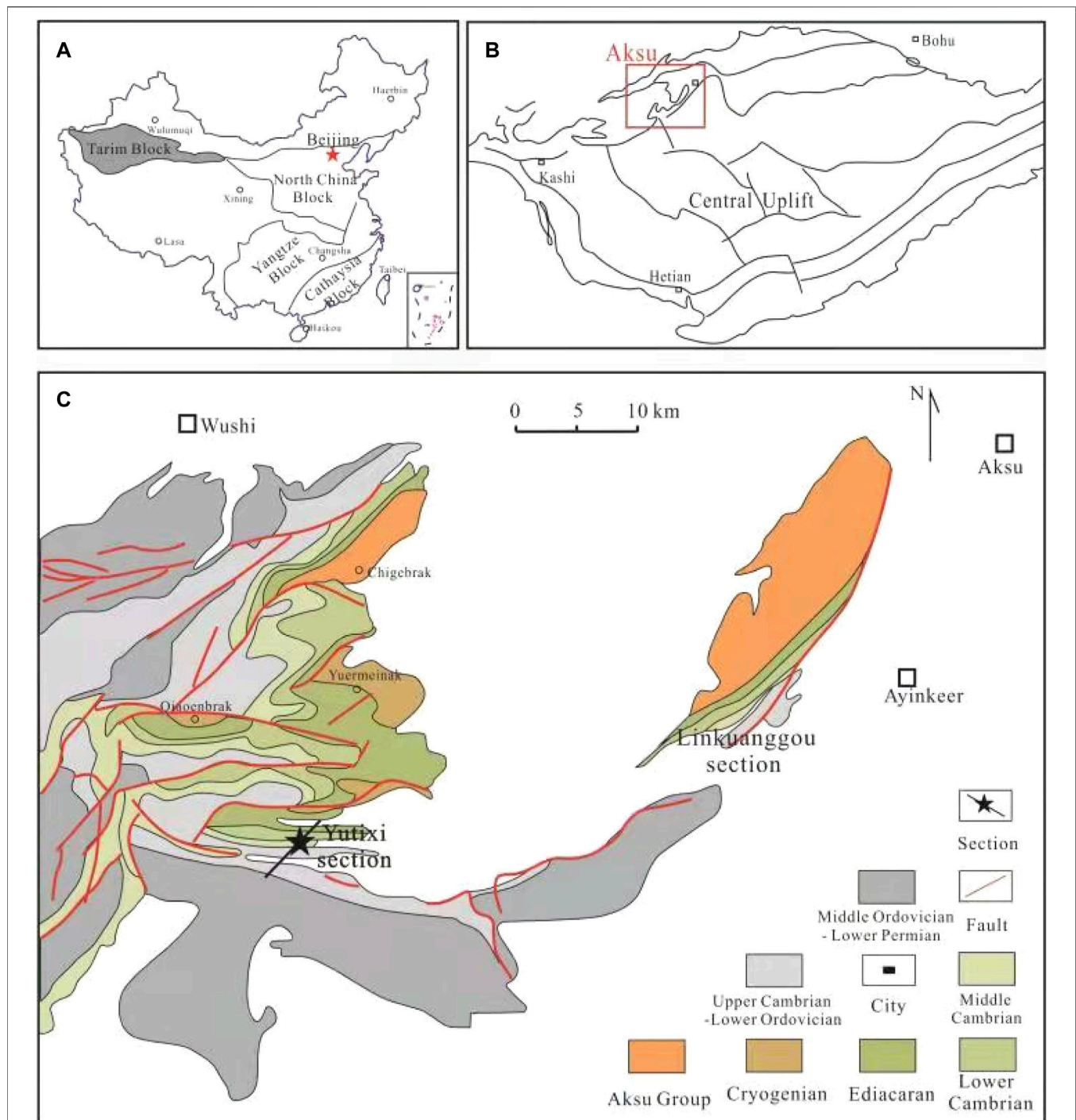


FIGURE 1 | (A) Geographic location of the Tarim Basin in northwestern China; (B) location map showing the tectonic units of the Tarim Basin and the Aksu area located in the northwest part of the Tarim Basin; (C) the field profile location of Aksu area, Tarim Basin (modified from Turner, 2010; Wen et al., 2015; Shen et al., 2022).

concentrations. The main steps are as follows: 1) weigh 50 mg sample (<200 mesh grain size) and put them into a clean and dry Teflon tank for sample dissolution; 2) add 1 ml HF, and heat to 150°C to remove Si from the samples; 3) after 1.0 ml HF and 0.6 ml HNO₃ were added, the Teflon tank should be placed in a steel jacket keeping at 190°C for more than 96 h. Then, the samples are

evaporated into emulsion droplets to remove excess HF; 4) after 1.6 ml HNO₃ is added, keep it at 140°C for 3–5 h; 5) the sample solution is transferred into a 50-ml centrifuge tube after cooling. Finally, 1 ml 500 PPB Rb (internal standard) is added into the centrifuge tube and diluted to 50 ml scale, and 6) sent to ICP-MS for testing.

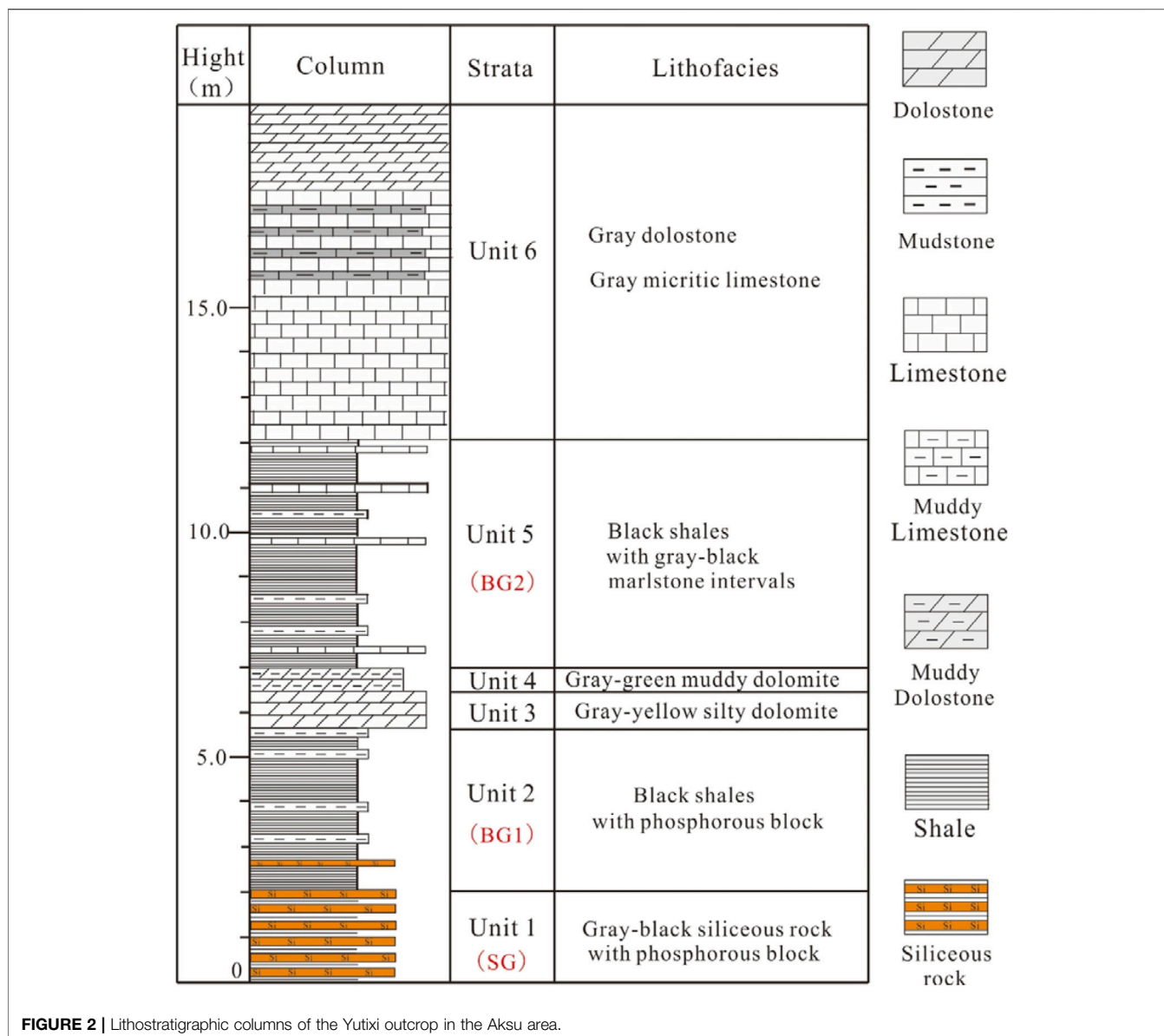


FIGURE 2 | Lithostratigraphic columns of the Yutixi outcrop in the Aksu area.

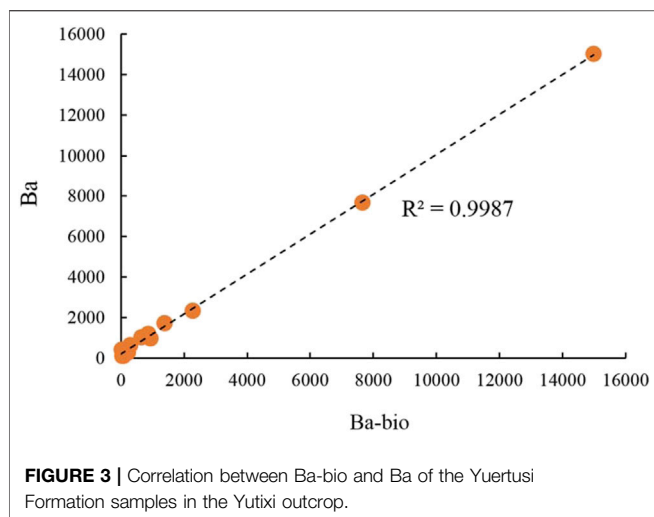
The rock powder (10 mg) was treated with 5% HCL at 80°C to remove inorganic carbon from samples. Then, these treated samples were washed with distilled water to fully remove the residual acid in the crucible, and these washed samples were dried in an oven at 70°C for 8 h. Finally, the iron powder and tungsten tin alloy were added to each sample as a combustion improver, and the total organic carbon (TOC) contents of samples were detected using the LECO CS230 elemental analyzer.

4 RESULTS

4.1 Major Elements

The major elements of the samples from the Yuertusi Formation in the Yutixi outcrop vary widely. The SiO₂ contents of the

samples from the Yuertusi Formation are relatively high, ranging from 4.10 to 95.12% (average of 47.12%). The contents of SiO₂ in SG are higher, ranging from 85.04 to 95.12%, with an average of 90.85%. The SiO₂ contents of BG1 are mostly above 50%, ranging from 7.28 to 58.19%, with an average of 49.35%. The SiO₂ contents of BG2 are relatively lower, ranging from 4.10 to 50.44%, with an average of 16.87%. In addition, the Al₂O₃ contents of SG are generally high, with an average of 9.62%, and those of BG1 are between 2 and 13%. The Fe₂O₃^T contents of the samples range from 0.22 to 4.34%, and the average value is 2.77%. The P₂O₅ contents of the samples from the Yuertusi Formation range from 0.01 to 3.55% (average of 0.53%), and the P₂O₅ contents of SG are generally higher than those of BG2. In addition, the contents of TiO₂, MnO, K₂O, PbO, and NaO are generally low.



4.2 Trace Elements

Trace elements in sediments were mainly derived from terrigenous clastic, authigenic minerals deposited by sediments or sedimentary water through chemical precipitation, *etc.* The presence of minerals of biogenic origin may dilute the abundance of trace elements in a sample. To eliminate this effect, it is customary to normalize the trace-element concentrations in terms of the Al or Th content, and express them as enrichment factors (EFs) (Riquier et al., 2006). The EFs of trace elements in each group are as follows: 1) SG: Ba > V > U > Mo > Cu > Sr > Cr > Zn > Pb; 2) BG1: Mo > Ba > U > V > Li > Cs > Cr > Ga > Rb; and 3) BG2: Mo > U > Zn > Pb > Sr > Li > Ba > Bi > Cu. Therefore, redox-sensitive elements such as Ba, Mo, V, U, Sr, Cr, Zn, and Cu are relatively enriched in the Yuertusi Formation.

4.3 Rare Elements

The total rare earth contents REE + Y of the Yuertusi Formation range from 12.61 $\mu\text{g/g}$ to 265.47 $\mu\text{g/g}$, with an average value of 126.06 $\mu\text{g/g}$. The REE + Y of BG1 range from 160.09 $\mu\text{g/g}$ to 265.47 $\mu\text{g/g}$, with an average value of 203.75 $\mu\text{g/g}$, which are much higher than those of SG and BG2. The REE + Y of SG range from 12.61 $\mu\text{g/g}$ to 121.43 $\mu\text{g/g}$, and the average value is 53.90 $\mu\text{g/g}$. LREE/HREE (the ratio of the heavy rare earth elements and the light rare earth elements) of BG1 ranges from 4.09 to 9.24, with an average of 6.37, which are much higher than those of SG and BG2. The LREE/HREE of SG is relatively lower, ranging from 0.86 to 1.28, with an average of 1.12.

5 DISCUSSION

5.1 The Paleo-Productivity

Marine paleo-productivity reflects the ability of organisms to produce or accumulate OM through assimilation, and it is impossible to measure the paleo-productivity directly (Algeo

et al., 2012; Zhang et al., 2016). Mostly, indirect measurements were carried out by establishing relations between parameters related to productivity. Barite in marine sediments and suspended particle is the main carrier of barium. According to its source, it can be divided into terrigenous clastic, biological (authigenic) genesis, hydrothermal precipitation, *etc.* Barium in biogenic barite is related to marine paleo-productivity (Tribovillard et al., 2006; Schoepfer et al., 2015), which is one of the reliable indicators for the reconstruction of paleo-productivity.

The significant correlation between total barium and biogenic barium in the Yuertusi Formation indicated that the changes of total barium were mainly caused by the biogenic barium (Figure 3). It showed obvious changes of biogenic barium (Figure 3); that is, the biogenic barium of SG is significantly higher than that of other groups. The samples are enriched with biogenic barium to varying degrees. In particular, the contents of biogenic barium in SG samples of the Yuertusi Formation are very high. The barium contents of BG1 and BG2 in the Yuertusi Formation indicate that there existed high paleo-productivity at the beginning of the Early Cambrian, but decreased at the end of the Early Cambrian. Although there are few samples with high TOC and Ba-bio, possibly due to the diluting, the high Ba-bio values suggest a high level of paleo-marine productivity in the Early Cambrian.

In addition to barium, other indicators including Cu, P, and Ba/Ti are also intuitive and effective for the reconstruction of paleo-productivity (Calvert and Pedersen, 2007). The Ba/Ti ratios vary with depths of the samples from the Yuertusi Formation, mainly ranging widely from 788.82 to 1666666.67, with an average value of 138854.75. The Ba/Ti ratio of the SG are relatively higher, with an average value of 758049.60; those of BG1 are moderate, with an average value of 7919.56; and those of BG2 decrease compared with SG and BG1, with an average value of 3021.20 (Figure 4). In general, the variations of the paleo-productivity indicators reflect a regular gradient from high paleo-productivity at its base to low paleo-productivity at its top, suggesting an upward-increasing paleo-productivity of the Yuertusi Formation. In addition, the parameters such as Cu and P also showed the same stratigraphic variations (Figure 4).

5.2 Mo–U Co-Variation and Mo/TOC

Mo–U co-variation and Mo/TOC are new indicators for paleo-environmental studies in recent years, which have been widely used to quantitatively study the retention and openness degree of paleo-marine (Tribovillard et al., 2008; Algeo et al., 2012). The EFs of Mo and U in paleo-marine were controlled by redox conditions and water circulation efficiency (Algeo and Maynard, 2004; Tribovillard et al., 2006; Algeo and Tribovillard, 2009). Due to their long retention time, Mo and U elements have similar concentrations in global oceans (Algeo and Tribovillard, 2009; Algeo et al., 2012). Mo exists in the form of stable MoO_4^{2-} in oxidized water. However, under anoxic conditions, Mo^{6+} will be reduced to activated Mo^{4+} (Zheng et al., 2000). In particular, in the presence of $\text{H}_2\text{S}/\text{HS}^-$, Mo^{4+} can combine with it to form

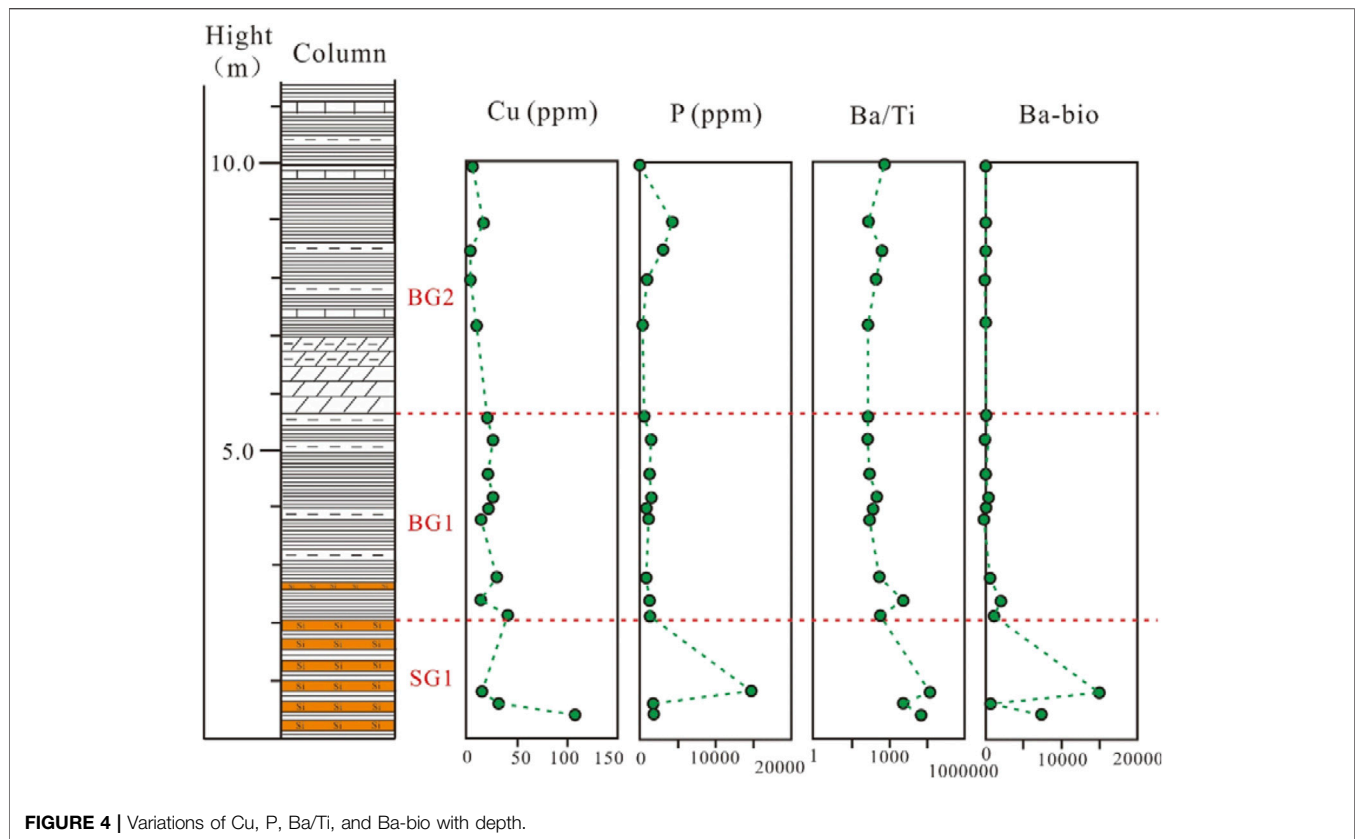


FIGURE 4 | Variations of Cu, P, Ba/Ti, and Ba-bio with depth.

highly activated thiomolybdate, which is eventually captured by ferromangous hydroxide or forms metal complexes with humic acid (Helz et al., 1996; Helz et al., 2011). Under the same reduction conditions, U can be activated in the Fe^{3+} - Fe^{2+} reduction band without the presence of $\text{H}_2\text{S}/\text{HS}^-$. Therefore, the differences of the chemical behavior of Mo and U elements under the reduction conditions can distinguish the sulfide degree in anoxic water (Tossell, 2005; Algeo and Tribovillard, 2009; Dellwig et al., 2010).

The black shales of the Yuertusi Formation in the study area show a variety of Mo–U co-variant modes, and all represent the positive co-variant characteristics of Mo_{EF} and U_{EF} (Figure 5A). Mo and U elements of SG samples show high degree of enrichment, and Mo/U values change greatly. The Mo/U values of BG1 samples are mainly between 1SW and 0.3SW; however, a few Mo/U values less than 0.3SW. It indicated that BG1 may be deposited in an anoxic environment, but sometimes, BG1 may be deposited in a hypoxic environment. The Mo/U values of BG2 samples are mainly between 1SW and 0.3SW; however, a few Mo/U values greater than 1SW, indicating that BG2 samples may be deposited in anoxic and sub-oxic environments. Mo concentration in sediments is consistent with the average value of Mo concentration of the global seawater. However, in restricted basins, the enhancement of seawater retention will increase the update time of Mo reservoir in seawater, which will lead to migration and loss of Mo ion (Tribovillard et al., 2008). The Mo–U co-variant chart showed that the Yuertusi

Formation mainly belonged to the unrestricted marine, and no samples consisted with a “particulate shuttle” (PS) trend (Figure 5A), indicating the high water circulation efficiency. Briefly, the Mo–U co-variant mode of the Yuertusi Formation in the study area had not corresponded to a modern ocean mode, but it roughly showed a trend parallel to the normal seawater covariant trend and fluctuated greatly.

In addition, Mo/TOC can be used to indicate the circulation efficiency and retention degree of paleo-marine (Algeo et al., 2012). The analysis shows that the Yuertusi Formation in the study area is characterized by Mo enrichment and low TOC (Figure 5B). There is a positive correlation between Mo and TOC, indicating that Mo was deposited in an anoxic environment. The ratios indicate that the circulation efficiency and retention degree of paleo-marine in the study area are mainly between those of the Sanich Gulf and Framvaren Fjord (Algeo and Lyons, 2006; Algeo et al., 2007). Therefore, as shallow water deposited under anoxic conditions and slight-moderate restriction, the black shales in the study area deposited in a semi-restricted bay lagoon environment with a small amount of seawater exchange.

5.3 Hydrothermal Activity

Studies suggest that REEs are mainly affected by different input sources such as river, weathering, and submarine hydrothermal, as well as the particle–solution interaction (Van Kranendonk et al., 2003; Nothdurft et al., 2004; Slack et al., 2007; Zhou et al.,

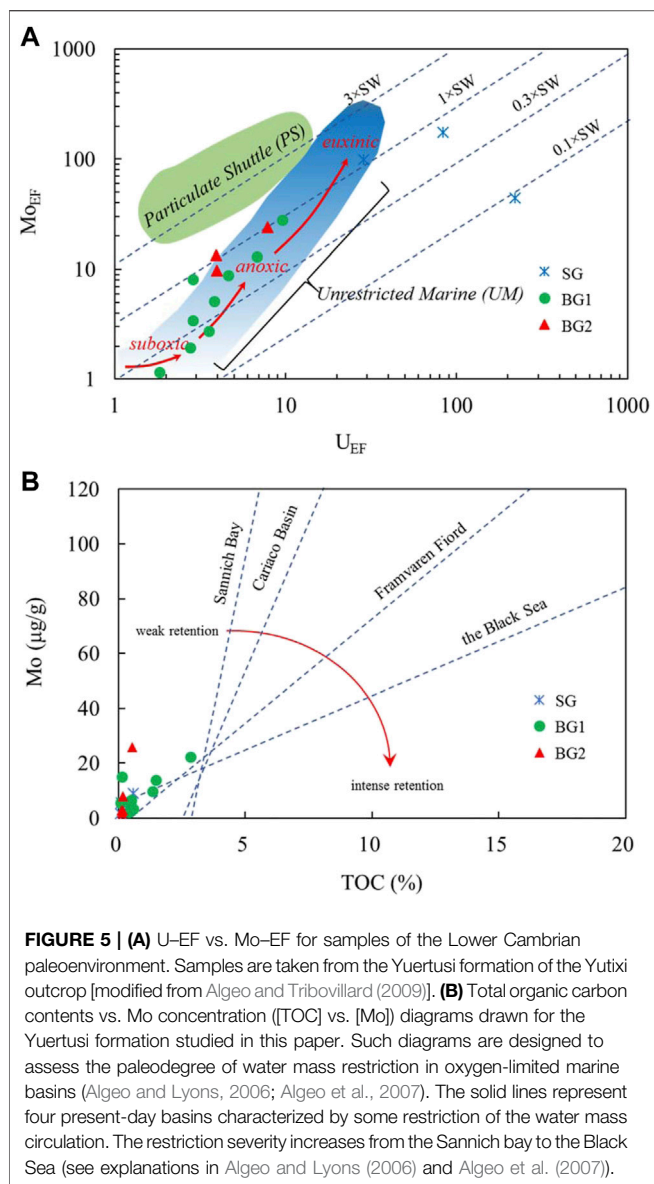


FIGURE 5 | (A) U-EF vs. Mo-EF for samples of the Lower Cambrian paleoenvironment. Samples are taken from the Yuertusi formation of the Yutixi outcrop [modified from Algeo and Tribouillard (2009)]. **(B)** Total organic carbon contents vs. Mo concentration ([TOC] vs. [Mo]) diagrams drawn for the Yuertusi formation studied in this paper. Such diagrams are designed to assess the paleodegree of water mass restriction in oxygen-limited marine basins (Algeo and Lyons, 2006; Algeo et al., 2007). The solid lines represent four present-day basins characterized by some restriction of the water mass circulation. The restriction severity increases from the Sannich bay to the Black Sea (see explanations in Algeo and Lyons (2006) and Algeo et al. (2007)).

2014). Compared with modern seawater, marine hydrothermal sediments generally show negative Ce/Ce^* anomalies ($Ce/Ce^* = Ce_N/(La_N \times Pr_N)^{1/2}$), low $\Sigma REEs$, and significant enrichment of heavy rare earth elements (Bau and Dulski, 1996) (Figure 6).

Generally, the LREE/HREE ratios of SG are significantly lower than those of BG1 and BG2. The average LREE/HREE ratios of SG, BG1, and BG2 are 1.12, 6.37, and 3.92, respectively (Figure 6), indicating that the REE of samples from SG is relatively depleted in LREE and enriched in HREE. The $\Sigma REEs$ of SG are low, with an average value of $33.04 \mu\text{g/g}$, which is much lower than that of the other two groups. SG shows a weak-moderate negative Ce anomaly, with an average Ce/Ce^* value of 0.57, while the average values of the other two groups are all greater than 0.90. According to the distribution diagram of $\Sigma REEs$, Ce/Ce^* , and LREE/HREE, it can be seen that

the SG of the Yuertusi Formation is of hydrothermal origin (Figure 6).

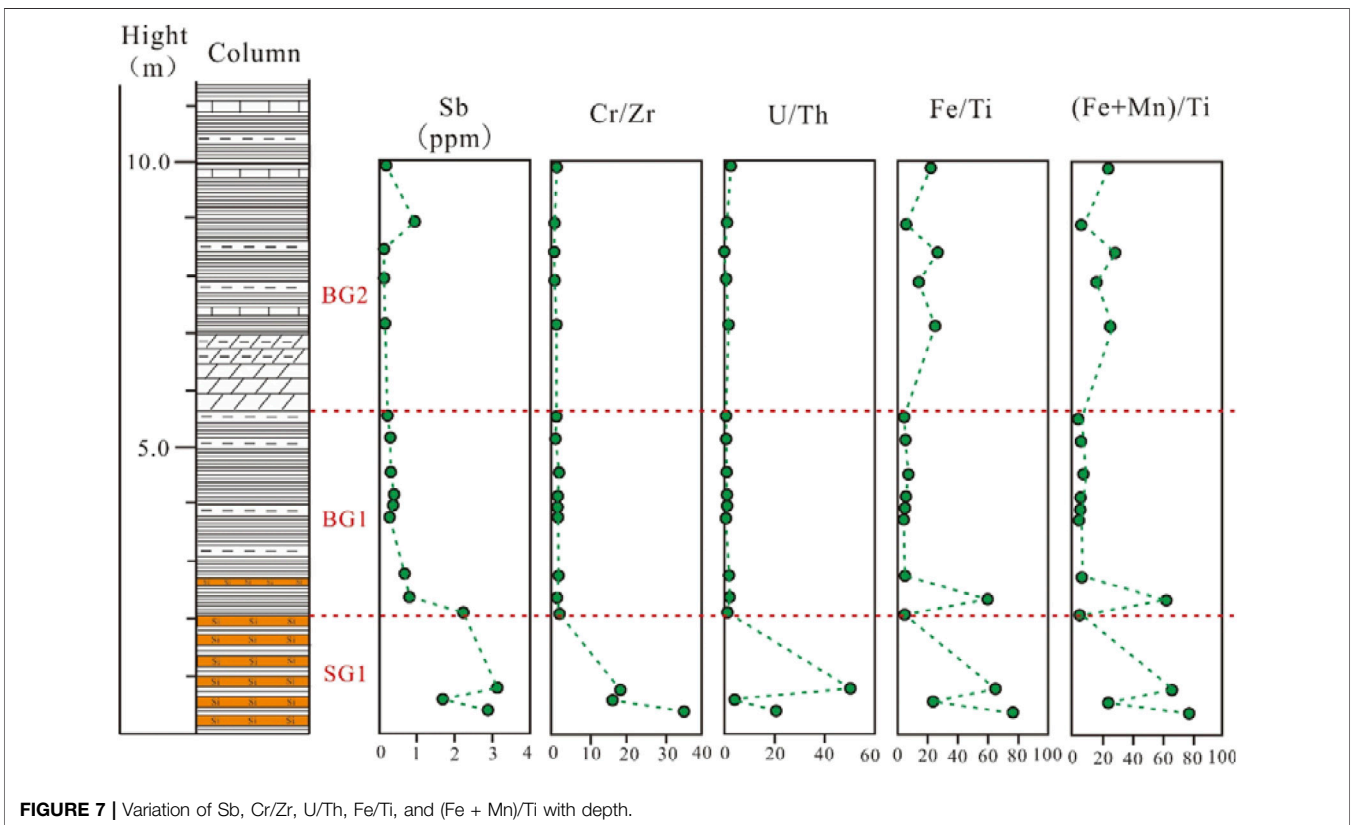
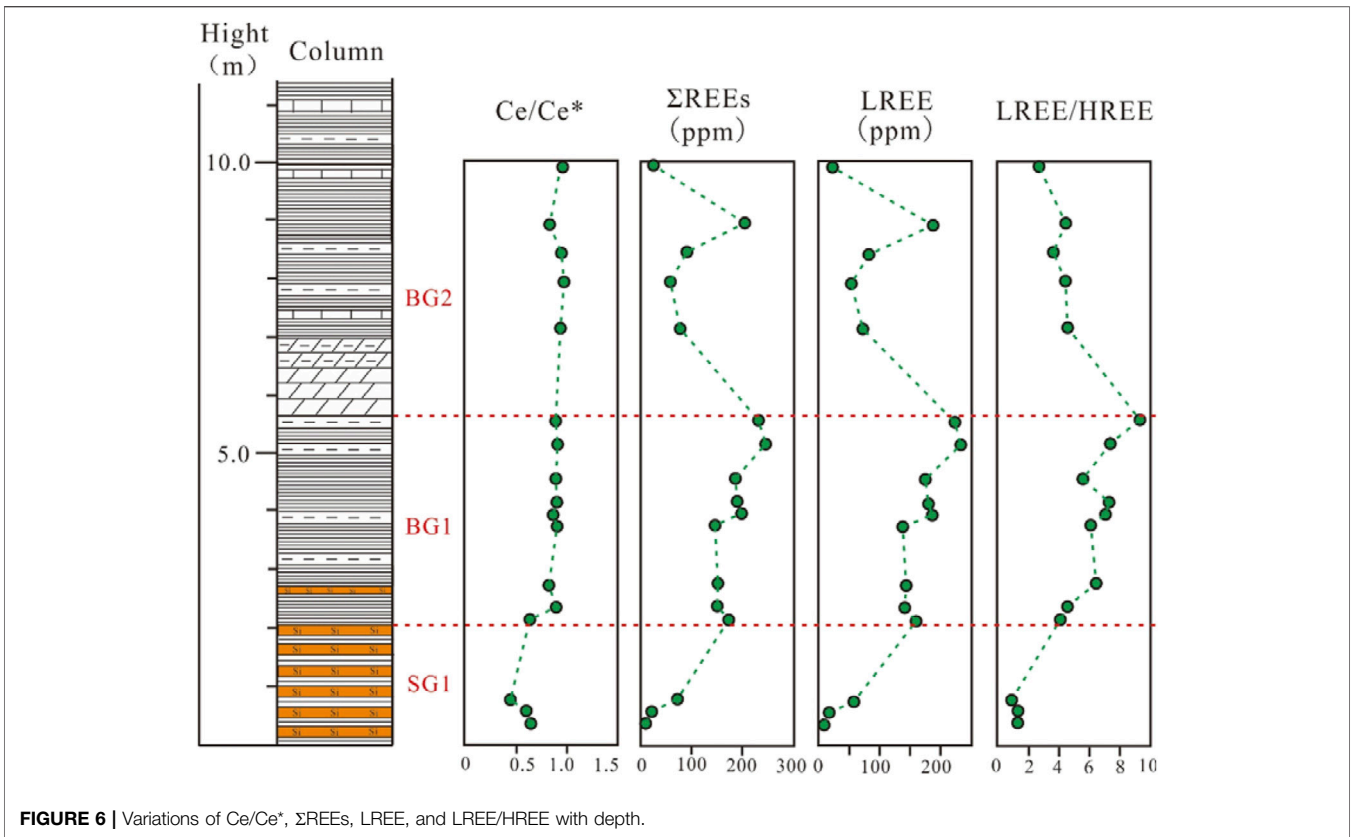
The seafloor hydrothermal solution can bring large amounts of Sb to the sediments (Rudnick and Gao, 2003). The contents of Sb in the SG and the BG1 are significantly higher, with an average of $2.45 \mu\text{g/g}$, which are much higher than the average content of Sb in the upper crust ($0.2 \mu\text{g/g}$). The Rb/Sr ratios of the SG are extremely low, close to the silicalite of hydrothermal origin (0.002) (Yu et al., 2004), and much lower than that of the upper crust (0.19) (Rudnick and Gao, 2003). In addition, hydrothermal activities are often closely related to life activities and microbial reproduction. The Cr/Zr values of SG are significantly higher than those of the other two groups, indicating obvious hydrothermal effects in the early deposition stage of the Yuertusi Formation. In addition, high U/Th is also considered as an important indicator for hydrothermal activities (Rudnick and Gao, 2003). Sediments with $U/Th > 1$ indicate hydrothermal origin, and sediments with $U/Th < 1$ indicate normal sedimentary origin (Rudnick and Gao, 2003). The U/Th ratio of marine silicalite is generally low, while the U/Th ratio is very high when the siliceous fluid comes from the deep crust or upper mantle. The U/Th ratios of SG in the Yuertusi Formation range from 4.01 to 49.69, with an average of 24.76, which are significantly higher than the U/Th ratio of the upper crust (0.23) (Rudnick and Gao, 2003), indicating the submarine hydrothermal origin.

In addition, the Fe/Ti and the $(Fe + Mn)/Ti$ ratios of the sediments can also be used as indicators to distinguish seafloor hydrothermal fluids. When $Fe/Ti > 20$ or $(Fe + Mn)/Ti > 20 \pm 5$, the sediments are considered as hydrothermal deposits (Boström, 1983). The average values of Fe/Ti and $(Fe + Mn)/Ti$ of the SG are 55.17 and 55.75, respectively, which are significantly larger than those of the SG and BG1 (Figure 7), indicating obvious submarine hydrothermal deposition.

The characteristics of trace elements of the SG in the Yuertusi Formation indicate that they were deposited by hydrothermal origin. The low TOC values of the SG (average of 0.24) may be caused by the intense hydrothermal activity, which brought a large amount of siliceous fluids and diluted the OM in the sediments. In other words, the intense hydrothermal activity damaged the development of the source rocks in the lower part of the Yuertusi Formation.

5.4 Trace Elements and Paleoenvironment

Trace elements are often absorbed on the surface of metal sulfides, insoluble oxides, phosphates, organometallic complexes, or organic compounds, and the enrichment degree of redox-sensitive trace elements is controlled by the redox state of seawater (Elderfield and Pagett, 1986; Sageman et al., 2003; Rimmer, 2004; Algeo and Lyons, 2006; Algeo and Rowe, 2012; Tribouillard et al., 2006; Robbins et al., 2016). Therefore, the redox state of the sedimentary environment can be judged by the contents or relative ratios of redox-sensitive elements such as Cr, V, U, and Ni (Jones and Manning, 1994; Kimura and Watanabe, 2001; Rimmer, 2004). The Th/U ratios of SG of the Yuertusi Formation are relatively lower, and all less than 1.33, with the average of 0.106. The Th/U ratios gradually increased upward in the Yuertusi Formation. The average Th/U ratios of BG1



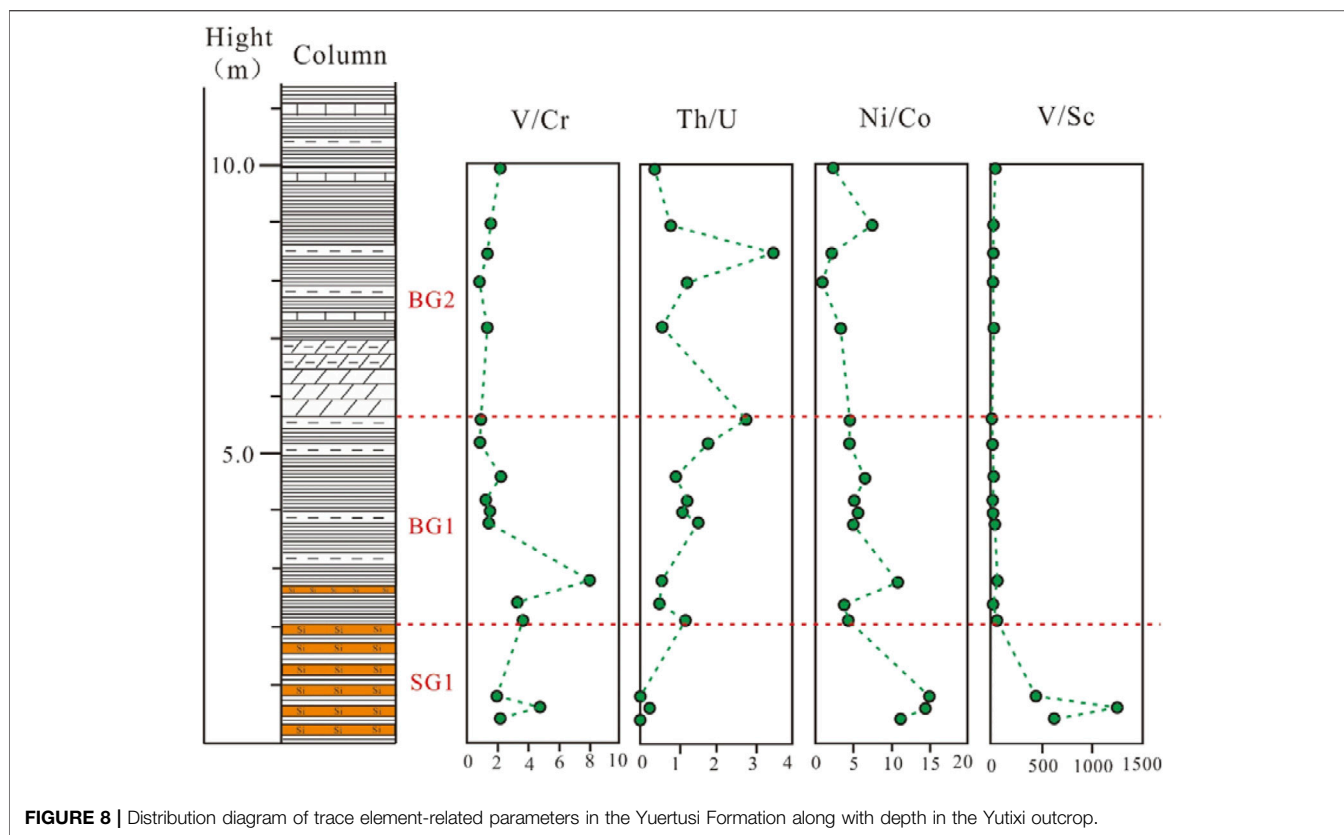


FIGURE 8 | Distribution diagram of trace element-related parameters in the Yuertusi Formation along with depth in the Yutixi outcrop.

and BG2 are 1.30 and 1.31, respectively. It generally indicated that the SG of the Yuertusi Formation was deposited in an obvious anoxic environment (Wignall and Twitchett, 1996; Kimura and Watanabe, 2001), and the seawater gradually oxidized upward (Figure 8). However, the Th/U values of the lower part of BG1 and BG2 are generally less than 1.33, but the values of the upper part of BG1 are generally more than 0.8, and even more than 1.33 at the top of the BG1 and the middle part of BG2. It reflected that the BG1 and BG2 of the Yuertusi Formation were deposited in an anoxic-suboxic environment with local oxidation. Similarly, the average V/Cr value of the samples from SG and the base of the BG1 was close to 4.0, and the V/Cr values of some samples reached 7.9 (Figure 8), indicating an intense reductive environment (Elderfield and Pagett, 1986). In addition, the results of Ni/Co and V/Sc values of the SG and the BG2 prove that it was deposited in a sulfide reduction environment (Rimmer, 2004) (Figure 8). In general, the silicalite of SG and the black shales at the base of BG1 were deposited in euxinic conditions, and the reduction degree was gradually weakened upward. The sedimentary paleoenvironment of the BG2 was more oxidized than that of BG1.

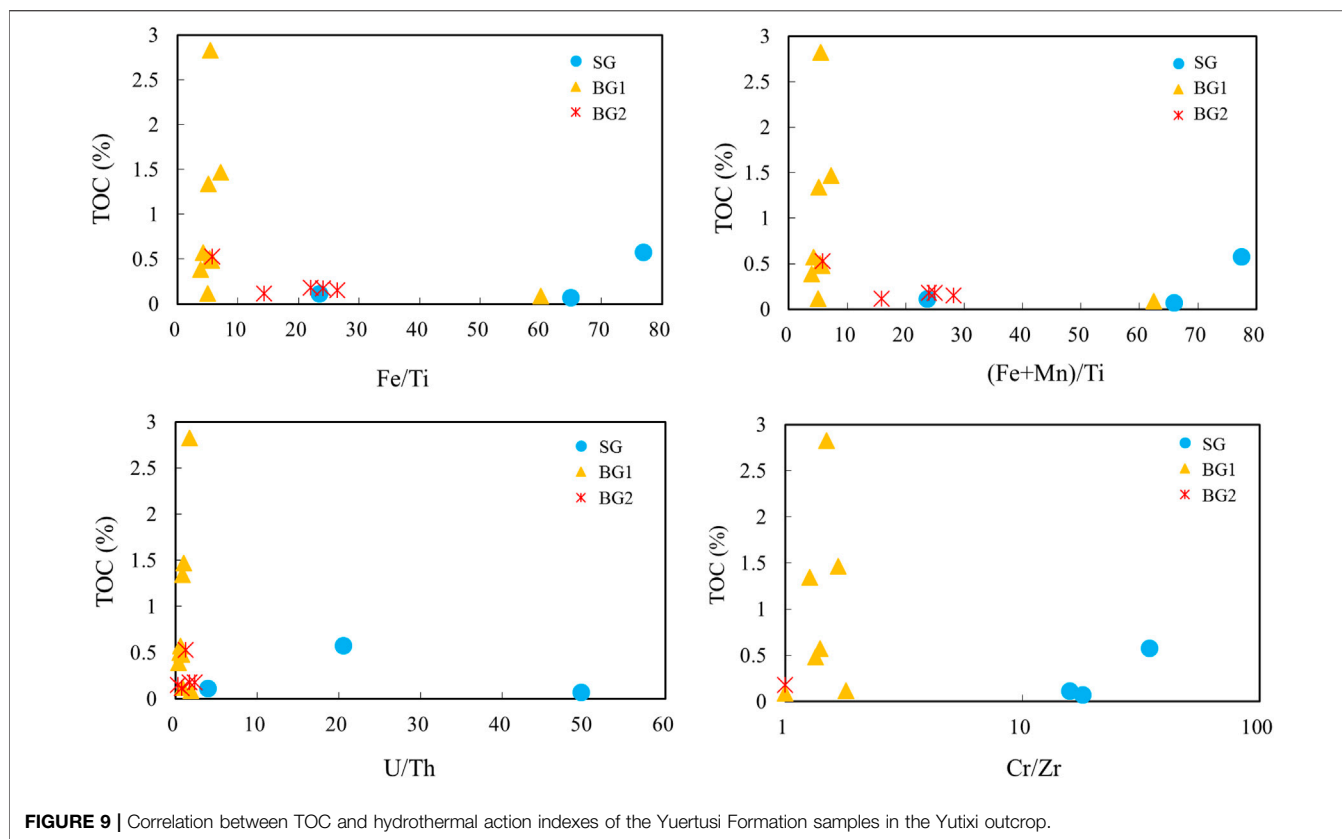
5.5 Formation Mechanism of the Source Rock

5.5.1 Paleoenvironment Controlling the OM Accumulation

TOC is usually used to evaluate the OM abundance of black shales (Guo, 2014). The range of TOC in the Yuertusi Formation

is 0.18–2.83%. In general, TOC of black shales in BG1 is the highest, and the values of some samples reach 2.83%. The correlation between TOC and hydrothermal indicator shows that OM accumulation is not significantly related to hydrothermal activity (Figure 9), which has not reflected that hydrothermal activity can promote the accumulation of OM in sediments.

There existed intense hydrothermal activity in the sedimentary period of SG, weak hydrothermal activity in the sedimentary period of the middle-lower part of BG1, and almost no hydrothermal activity in the sedimentary period of the BG2 and upper part of BG1. Although hydrothermal activity in the SG contributed to the increase of paleo-productivity, the TOC value was relatively low, ranging from 0.07 to 0.57%, with an average of 0.25%. BG1 is the main source rock with the highest TOC of the Yuertusi Formation. Previous studies (Chu et al., 2016) showed that the silicalite associated with hydrothermal activity in the Yuertusi Formation contained a large number of algae. The intense hydrothermal activity brought a large number of silica-rich fluids and diluted the OM in the sediments, which destroyed the formation of source rocks. Through the study on the geochemistry of the Yuertusi Formation, Ouyang et al. (2022) found that the weak hydrothermal activity was more conducive to the accumulation of OM than the intense hydrothermal activity and the non-hydrothermal activity. BG1, the first set of black shales, was deposited in a weak hydrothermal environment, which was more conducive to the accumulation of OM.



According to the correlation diagram analyses of Ni/Co, V/Cr, V/(V + Ni), V/Sc, and TOC, enrichment degrees of OM in different layers of the Yuertusi Formation are different under the influence of redox conditions (**Figure 10**). The Ni/Co, V/Cr, V/(V + Ni), and V/Sc redox indexes of SG have no significant correlation with TOC, and the redox indexes of SG indicate that the deposition environment of SG is the most reductive. However, this did not result in a large TOC of SG. The Ni/Co, V/Cr, V/(V + Ni), and V/Sc redox indexes of BG1 and BG2 are positively correlated with TOC, indicating that OM accumulation in two sets of black shales was affected by redox conditions, and the enhanced reducibility of paleoenvironment was conducive to OM accumulation. The depositional environment of BG1 is more reductive than that of BG2, which is more conducive to OM accumulation, so the TOC of BG1 is higher than that of BG2.

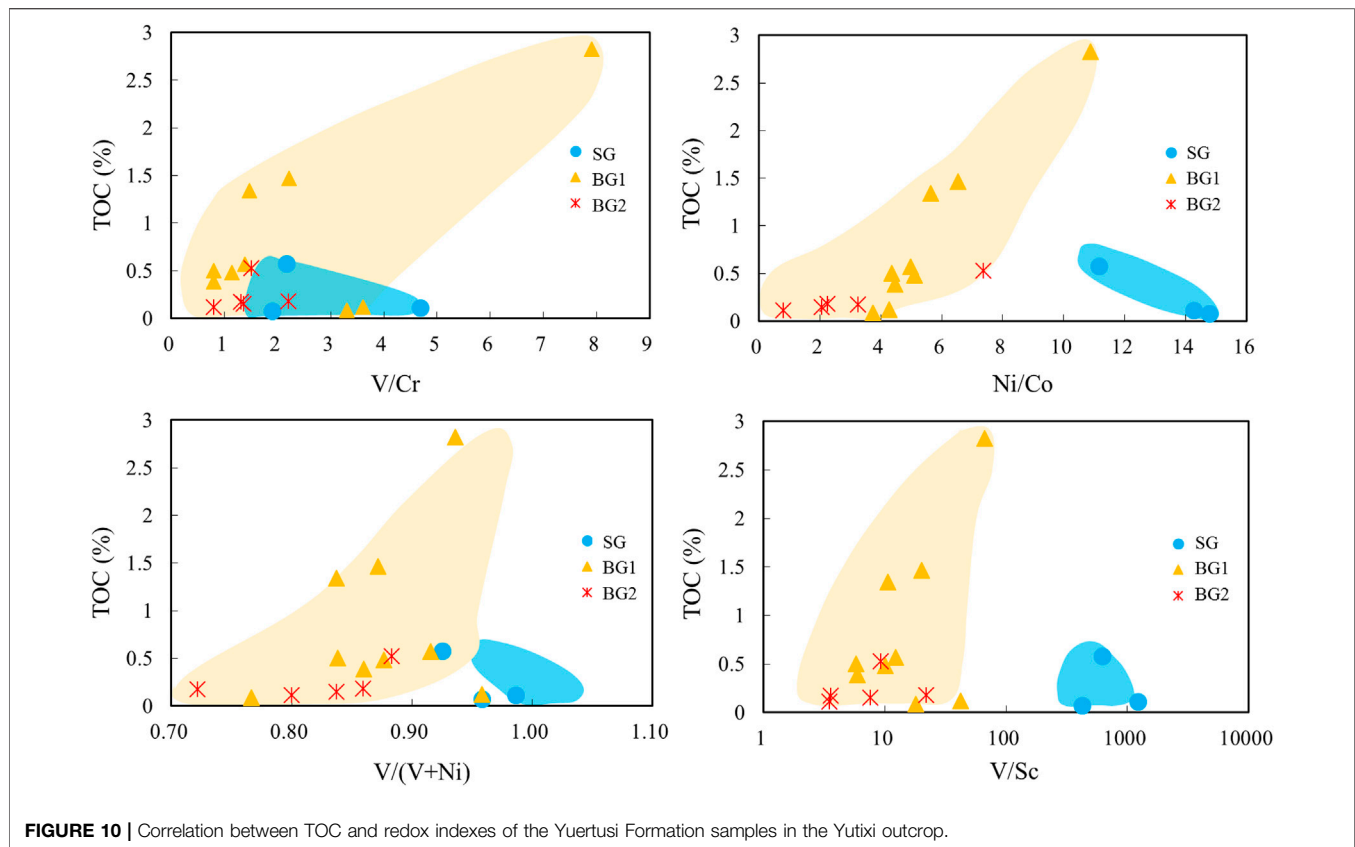
5.5.2 OM Accumulation Model

In general, OM accumulation of the Yuertusi Formation in the Yutixi outcrop is controlled by hydrothermal activity and paleo-marine redox conditions. Based on the redox conditions traced by U/Th, V/Cr, and Ni/V; the hydrothermal activity traced by Ce/Ce⁺, Cr/Zr, U/Th, Fe/Ti, and (Fe + Mn)/Ti ratio; and paleo-productivity traced by Ba, Cu, Rb/Sr, and other parameters, variations were observed in the depositional environments of the Yuertusi Formation.

In the sedimentary period of SG, the paleo-marine was dominated by euxinic environment, and the reduction degree of the paleo-marine during the sedimentary period of SG was the strongest. However, the TOC values of SG were very low. When the SG of the Yuertusi Formation was deposited, the study area began transgression with intense hydrothermal activity, which greatly improved the marine paleo-productivity. However, the intense hydrothermal activity brought a large amount of silica-rich fluids and diluted the OM in the sediments, leading to the destruction of source rocks. The results showed that although the SG was deposited in a highly reductive environment, the dilution of hydrothermal activity obviously destroyed the accumulation of OM in SG.

During the sedimentary period of black shales in the BG1, the paleo-marine was dominated by oxygen-poor environment, and the redox indexes and TOC show good positive correlations, indicating that the anoxic environment provided effective conditions for the preservation of OM. The hydrothermal activity in the study area was relatively weak during the sedimentary period of BG1, which was more conducive to the accumulation of OM than the intense hydrothermal activity and not hydrothermal activity. Therefore, as the layer with the maximum TOC value of the Yuertusi Formation in the study area, the OM accumulation of SG may be controlled by the comprehensive control of biological productivity and redox state.

During the sedimentary period of black shales in the BG2, the paleo-marine began to retreat and the sedimentary water became



shallower. The reduction degree of seawater decreased, which was characterized by poor to partial oxidation environment, and it was not conducive to the preservation of OM. The hydrothermal activity was further weakened relative to the SG and BG1, and the paleo-productivity continued to decline. Therefore, low productivity and oxidizing environment led to the low TOC in this period.

6 CONCLUSION

- 1) The Yuertusi Formation from the Yutixi outcrop in the Aksu area can be divided into six layers, from old to young: gray-black thin silicalite, black shales interbedded with silica thin bedded, gray-yellow silty dolomite, gray-green silty clastic dolomite, black shales interbedded with gray-black thin bedded marl, and gray thin micritic limestone, forming a complete transgression–regression sedimentary cycle.
- 2) Seawater oxygenation and decreasing-upward primary production were recorded in the Yuertusi Formation: 1) the silicalite at the base was deposited in the unrestricted marine environment with euxinic conditions and intense hydrothermal activity, 2) the lower black shales were deposited in oxygen-poor conditions with weak hydrothermal activity, and 3) the upper black shales were deposited in oxygen-poor and sub-oxidized conditions with

local oxic conditions, and there was almost no hydrothermal activity.

- 3) An “integrated model” for OM accumulation in the Yuertusi Formation can be established: 1) Primary production provided material source for OM accumulation; 2) redox conditions were conducive to OM preservation. The anoxic conditions, controlling the preservation of OM, and the appropriate hydrothermal activities, improving primary production, jointly controlled the formation of high-quality source rocks represented by the black shales of the Yuertusi Formation, especially the first set of black shales.

DATA AVAILABILITY STATEMENT

The original contributions presented in the study are included in the article/Supplementary Material, further inquiries can be directed to the corresponding author.

AUTHOR CONTRIBUTIONS

YW and WS designed the project; YW and WS did the fieldwork and collected samples; YW and ML performed geochemical analyses; JC and WS interpreted the data. YW and WS wrote the paper, with additional input from all the coauthors.

FUNDING

This work was supported by the National Natural Science Foundation of China (Grant No 42002161).

REFERENCES

- Algeo, T. J., Lyons, T. W., Blakey, R. C., and Over, D. J. (2007). Hydrographic Conditions of the Devonian-Carboniferous North American Seaway Inferred from Sedimentary Mo-TOC Relationships. *Palaeoogeogr. Palaeoeclimatol. Palaeoecol.* 256, 204–230. doi:10.1016/j.palaeo.2007.02.035
- Algeo, T. J., Morford, J., and Cruse, A. (2012). New Applications of Trace Metals as Proxies in Marine Paleoenvironments. *Chem. Geology.* 306–307, 160–164. doi:10.1016/j.chemgeo.2012.03.009
- Algeo, T. J., and Lyons, T. W. (2006). Mo-total Organic Carbon Covariation in Modern Anoxic marine Environments: Implication for Analysis of Paleoredox and Paleo-hydrographic Conditions. *Paleoceanography* 21, PA1016. doi:10.1029/2004pa001112
- Algeo, T. J., and Maynard, J. B. (2004). Trace-element Behavior and Redox Facies in Core Shales of Upper Pennsylvanian Kansas-type Cyclothems. *Chem. Geology.* 206, 289–318. doi:10.1016/j.chemgeo.2003.12.009
- Algeo, T. J., and Rowe, H. (2012). Paleocceanographic Applications of Trace-Metal Concentration Data. *Chem. Geology.* 324–325, 6–18. doi:10.1016/j.chemgeo.2011.09.002
- Algeo, T. J., and Tribouillard, N. (2009). Environmental Analysis of Paleocceanographic Systems Based on Molybdenum-Uranium Covariation. *Chem. Geology.* 268, 211–225. doi:10.1016/j.chemgeo.2009.09.001
- Bau, M., and Dulski, P. (1996). Distribution of Yttrium and Rare-earth Elements in the Penge and Kuruman Iron-formations, Transvaal Supergroup, South Africa. *Precambrian Res.* 79 (1–2), 37–55. doi:10.1016/0301-9268(95)00087-9
- Boström, K. (1983). *Genesis of Ferromanganese Deposits-Diagnostic Criteria for Recent and Old deposits Hydrothermal Processes at Seafloor Spreading Centers.* New York: Springer, 473–489.
- Calvert, S. E., and Pedersen, T. F. (2007). Chapter Fourteen Elemental Proxies for Palaeoclimatic and Palaeoceanographic Variability in Marine Sediments: Interpretation and Application. *Dev. Mar. Geology.* 1, 567–644. doi:10.1016/s1572-5480(07)01019-6
- Chen, Q., Chu, C., Yang, X., Hu, G., Shi, Z., Jiang, H., et al. (2015). Sedimentary Model and Development of the Cambrian Source Rocks in the Tarim Basin, NW China. *Petrol. Geol. Exp.* 37, 689–695. (in Chinese with English abstract). doi:10.11781/syzydz201506689
- Chu, C. L., Chen, Q. L., and Zhang, B. (2016). Influence on Formation of Yuertusi Source Rock by Hydrothermal Activities at Dongergou Section, Tarim Basin. *Acta sedimentologica sinica* 34, 803–810. (in Chinese with English abstract). doi:10.14027/j.cnki.cjxb.2016.04.020
- Chunyu Zhang, C., Guan, S., Wu, L., Ren, R., Wang, L., and Wu, X. (2020). Depositional Environments of Early Cambrian marine Shale, Northwestern Tarim Basin, China: Implications for Organic Matter Accumulation. *J. Pet. Sci. Eng.* 194, 107497. doi:10.1016/j.petrol.2020.107497
- Dellwig, O., Leipe, T., März, C., Glockzin-Pollehne, M., Pollehne, F., Schnetger, B., et al. (2010). A New Particulate Mn-Fe-P-Shuttle at the Redoxcline of Anoxic Basins. *Geochimica et Cosmochimica Acta* 74, 7100–7115. doi:10.1016/j.gca.2010.09.017
- Dong, L., Xiao, S., Shen, B., Zhou, C., Li, G., and Yao, J. (2009). Basal Cambrian Microfossils from the Yangtze Gorges Area (South China) and the Aksu Area (Tarim Block, Northwestern China). *J. Paleontol.* 83, 30–44. doi:10.1666/07-147r.1
- Elderfield, H., and Pagett, R. (1986). Rare Earth Elements in Ichthyoliths: Variations with Redox Conditions and Depositional Environment. *Sci. Total Environ.* 49 (86), 175–197. doi:10.1016/0048-9697(86)90239-1
- Guo, L. (2014). *Geological Characteristics and Shale Gas prospect Evaluation of Lower Cambrian Black Shale in the Upper Yangtze basin.* Chengdu: Chengdu University of Technology.
- Guo, Q., Deng, Y., Hu, J., and Wang, L. (2017). Carbonate Carbon Isotope Evolution of Seawater across the Ediacaran-Cambrian Transition: Evidence from the Keping Area, Tarim Basin, NW China. *Geol. Mag.* 154, 1244–1256. doi:10.1017/s0016756817000206
- He, D., Jia, C., Li, D., Zhang, C., Meng, Q., and Shi, X. (2005). Formation and Evolution of Polycyclic Superimposed Tarim Basin. *Oil Gas Geol.* 26, 64–77. (in Chinese with English abstract).
- Helz, G. R., Miller, C. V., Charnock, J. M., Mosselmans, J. F. W., Patrick, R. A. D., Garner, C. D., et al. (1996). Mechanism of Molybdenum Removal from the Sea and its Concentration in Black Shales: EXAFS Evidence. *Geochimica et Cosmochimica Acta* 60, 3631–3642. doi:10.1016/0016-7037(96)00195-0
- Helz, G. R., Bura-Nakić, E., Mikac, N., and Ciglenčki, I. (2011). New Model for Molybdenum Behavior in Euxinic Waters. *Chem. Geology.* 284, 323–332. doi:10.1016/j.chemgeo.2011.03.012
- Hu, G., Meng, Q., Wang, J., Tengger, X. X., Lu, L., and Liu, W. (2018). The Original Organism Assemblages and Kerogen Carbon Isotopic Compositions of the Early Paleozoic Source Rocks in the Tarim Basin, China. *Acta Geol. Sin.-engl.* 92, 2297–2309. doi:10.1111/1755-6724.13729
- Jia, C., and Wei, G. (2002). Structural Characteristics and Petroliferous Features of Tarim Basin. *Chin. Sci. Bull.* 47, 1–11. (in Chinese with English abstract). doi:10.1007/bf02902812
- Jin, Z., Tan, X., Tang, H., Shen, A., Qiao, Z., Zheng, J., et al. (2020). Sedimentary Environment and Petrological Features of Organic-Rich fine Sediments in Shallow Water Overlapping Deposits: a Case Study of Cambrian Yuertus Formation in Northwestern Tarim Basin, NW China. *Petrol. Explor. Dev.* 47, 476–489. (in Chinese with English abstract). doi:10.1016/s1876-3804(20)60069-6
- Jones, B., and Manning, D. A. C. (1994). Comparison of Geochemical Indices Used for the Interpretation of Palaeoredox Conditions in Ancient Mudstones. *Chem. Geology.* 111, 111–129. doi:10.1016/0009-2541(94)90085-x
- Kimura, H., and Watanabe, Y. (2001). Oceanic Anoxia at the Precambrian-Cambrian Boundary. *Geol.* 29, 995–998. doi:10.1130/0091-7613(2001)029<0995:oaatpc>2.0.co;2
- Kun Zhang, K., Jia, C., Song, Y., Jiang, S., Jiang, Z., Wen, M., et al. (2020). Analysis of Lower Cambrian Shale Gas Composition, Source and Accumulation Pattern in Different Tectonic Backgrounds: A Case Study of Weiyuan Block in the Upper Yangtze Region and Xiuwu Basin in the Lower Yangtze Region. *Fuel* 263 (2020), 115978. doi:10.1016/j.fuel.2019.115978
- Lan, Z., Li, X.-H., Chu, X., Tang, G., Yang, S., Yang, H., et al. (2017). SIMS U-Pb Zircon Ages and Ni-Mo-PGE Geochemistry of the Lower Cambrian Niutitang Formation in South China: Constraints on Ni-Mo-PGE Mineralization and Stratigraphic Correlations. *J. Asian Earth Sci.* 137, 141–162. doi:10.1016/j.jseas.2016.12.046
- Li, X., Zhang, J., Wang, Y., Guo, M., Wang, Z., and Wang, F. (2018). Accumulation Condition and Favorable Area Evaluation of Shale Gas from the Niutitang Formation in Northern Guizhou, South China. *J. Nat. Gas Geosci.* 3, 1–10. doi:10.1016/j.jnggs.2018.03.001
- Liu, W., Zhang, G., Pan, W., Deng, S., and Li, H. (2011). Lithofacies Palaeogeography and Sedimentary Evolution of the Cambrian in Tarim Area. *J. Palaeoogeogr.* 13, 529–538. (in Chinese with English abstract).
- Nothdurft, L. D., Webb, G. E., and Kamber, B. S. (2004). Rare Earth Element Geochemistry of Late Devonian Reefal Carbonates, Canning Basin, Western Australia: Confirmation of a Seawater REE Proxy in Ancient Limestones. *Geochimica et Cosmochimica Acta* 68, 263–283. doi:10.1016/s0016-7037(03)00422-8
- Ouyang, S. Q., Lv, X. X., Xue, L., et al. (2022). Paleoenvironmental Characteristics and Source Rock Development Model of the Early-Middle Cambrian: A Case of the Keping-Bachu Area in the Tarim Basin. *J. China Univ. Mining & Technology* 51, 239–256. doi:10.13247/j.cnki.jcmt.001335
- Pan, W., Chen, Y., Xiong, Y., Li, B., and Xiong, R. (2015). Sedimentary Facies Research and Implications to Advantaged Exploration Regions on Lower Cambrian Source Rocks, Tarim Basin. *Nat. Gas Geosci.* 26, 1224–1232. (in Chinese with English abstract). doi:10.11764/j.issn.1672-1926.2015.07.1224
- Rimmer, S. M. (2004). Geochemical Paleoredox Indicators in Devonian-Mississippian Black Shales, Central Appalachian Basin (USA). *Chem. Geology.* 206, 373–391. doi:10.1016/j.chemgeo.2003.12.029
- Robbins, L. J., Lalonde, S. V., Planavsky, N. J., Partin, C. A., Reinhard, C. T., Kendall, B., et al. (2016). Trace Elements at the Intersection of marine Biological

ACKNOWLEDGMENTS

The authors are particularly grateful to Editor KZ and the reviewers for their constructive reviews and comments on the manuscript.

- and Geochemical Evolution. *Earth-Science Rev.* 163, 323–348. doi:10.1016/j.earscirev.2016.10.013
- Rudnick, R. L., and Gao, S. (2003). “Composition of the Continental Crust,” *Treatise on Geochemistry*. Editor R. L. Rudnick (Amsterdam: Elsevier Oxford), Vol. 3, 1–64. (Pergamon). doi:10.1016/b0-08-043751-6/03016-4
- Ryu, J.-S., Jacobson, A. D., Holmden, C., Lundstrom, C., and Zhang, Z. (2011). The Major Ion, $\delta^{44}/^{40}\text{Ca}$, $\delta^{44}/^{42}\text{Ca}$, and $\delta^{26}/^{24}\text{Mg}$ Geochemistry of Granite Weathering at pH=1 and T=25°C: Power-Law Processes and the Relative Reactivity of Minerals. *Geochimica et Cosmochimica Acta* 75, 6004–6026. doi:10.1016/j.gca.2011.07.025
- Sageman, B. B., Murphy, A. E., Werne, J. P., Ver Straeten, C. A., Hollander, D. J., and Lyons, T. W. (2003). A Tale of Shales: the Relative Roles of Production, Decomposition, and Dilution in the Accumulation of Organic-Rich Strata, Middle–Upper Devonian, Appalachian basin. *Chem. Geology*. 195 (1–4), 229–273. doi:10.1016/s0009-2541(02)00397-2
- Schoepfer, S. D., Shen, J., Wei, H., Tyson, R. V., Ingall, E., and Algeo, T. J. (2015). Total Organic Carbon, Organic Phosphorus, and Biogenic Barium Fluxes as Proxies for Paleomarine Productivity. *Earth-Science Rev.* 149, 23–52. doi:10.1016/j.earscirev.2014.08.017
- Shen, W., Zhu, X., Xie, H., Wang, X., and He, Y. (2022). Tectonic-sedimentary Evolution during Initiation of the Tarim Basin: Insights from Late Neoproterozoic Sedimentary Records in the NW basin. *Precambrian Res.* 371, 106598. doi:10.1016/j.precamres.2022.106598
- Slack, J. F., Grenne, T., Bekker, A., Rouxel, O. J., and Lindberg, P. A. (2007). Suboxic Deep Seawater in the Late Paleoproterozoic: Evidence from Hematitic Chert and Iron Formation Related to Seafloor-Hydrothermal Sulfide Deposits, Central Arizona, USA. *Earth Planet. Sci. Lett.* 255 (1–2), 243–256. doi:10.1016/j.epsl.2006.12.018
- Tossell, J. A. (2005). Calculating the Partitioning of the Isotopes of Mo between Oxidic and Sulfidic Species in Aqueous Solution. *Geochimica et Cosmochimica Acta* 69, 2981–2993. doi:10.1016/j.gca.2005.01.016
- Tribouillard, N., Algeo, T. J., Lyons, T., and Riboulleau, A. (2006). Trace Metals as Paleoredox and Paleoproductivity Proxies: an Update. *Chem. Geology*. 232, 12–32. doi:10.1016/j.chemgeo.2006.02.012
- Tribouillard, N., Bout-Roumazilles, V., Algeo, T. J., Lyons, T. W., Sionneau, T., Montero Serrano, J. C., et al. (2008). Paleodepositional Conditions in the Orca Basin as Inferred From organic Matter and Trace Metal Contents. *Mar. Geology*. 254 (1/2), 62–72. doi:10.1016/j.margeo.2008.04.016
- Turner, S. A. (2010). Sedimentary Record of Late Neoproterozoic Rifting in the NW Tarim Basin. *China. Precambrian Res.* 181 (1–4), 85–96. doi:10.1016/j.precamres.2010.05.015
- Van Kranendonk, M. J., Webb, G. E., and Kamber, B. S. (2003). Geological and Trace Element Evidence for a marine Sedimentary Environment of Deposition and Biogenicity of 3.45 Ga Stromatolitic Carbonates in the Pilbara Craton, and Support for a Reducing Archaean Ocean. *Geobiology* 1, 91–108. doi:10.1046/j.1472-4669.2003.00014.x
- Wen, B., Evans, D. A. D., Li, Y.-X., Wang, Z., and Liu, C. (2015). Newly Discovered Neoproterozoic Diamictite and Cap Carbonate (DCC) Couplet in Tarim Craton, NW China: Stratigraphy, Geochemistry, and Paleoenvironment. *Precambrian Res.* 271, 278–294. doi:10.1016/j.precamres.2015.10.006
- Wignall, P. B., and Twitchett, R. J. (1996). Oceanic Anoxia and the End Permian Mass Extinction. *Science* 272 (5265), 1155–1158. doi:10.1126/science.272.5265.1155
- Wu, G. H., Li, H. H., Zhang, L. P., Wang, C., and Zhou, B. (2012). Reservoir-forming Conditions of Ordovician Weathering Crust in Maigaiti Slope, Tarim Basin. *Pet. Exploration Dev.* 2, 144–153.
- Yang, Z. Y., Luo, P., Liu, B., Liu, C., Ma, J., and Chen, F. R. (2017). Differences and Genesis of Two Sets of Black Rock Series of Lower Cambrian Yuertusi Formation in Aksu Area, Tarim Basin. *Acta Petrologica Sinica* 33 (06), 1893–1918. (in Chinese with English abstract).
- Yao, C. Y., Ma, D. S., Ding, H. F., and Zhang, X. Y. (2011). Early Cambrian Carbonate Sedimentary Environment in Aksu Area, Xinjiang: Trace Elements and Carbon Isotope Evidence. *Geochimica* 40, 63–71. (in Chinese with English abstract). doi:10.19700/j.0379-1726.2011.01.007
- Yao, C., Ma, D., Ding, H., Zhang, X., and Huang, H. (2014). Trace Elements and Stable Isotopic Geochemistry of an Early Cambrian Chert-Phosphorite Unit from the Lower Yuertusi Formation of the Sugetbrak Section in the Tarim Basin. *Sci. China Earth Sci.* 57, 454–464. doi:10.1007/s11430-013-4760-9
- Yao, C., Guo, W., Liu, J., and Li, H. (2017). Multiple Proxies on the Paleoenvironment of the Early Cambrian marine Black Rock Series in the Tarim Basin, NW China: Molybdenum Isotope and Trace Element Evidence. *Int. J. Geosciences* 08, 965–983. doi:10.4236/ijg.2017.88055
- Yu, B. S., Chen, J. Q., Li, X. W., and Lin, C. S. (2004). The Siliceous Microfacies of the Lower Cambrian in the Xiaoqbulak Section, Tarim Basin Geochemistry of Quantitative Elements and Rare Earth Elements and Their Sedimentary Setting. *Acta Sedimentologica Sinica* 2004 (1), 59–66.
- Yu, B., Dong, H., Widom, E., Chen, J., and Lin, C. (2009). Geochemistry of Basal Cambrian Black Shales and Cherts from the Northern Tarim Basin, Northwest China: Implications for Depositional Setting and Tectonic History. *J. Asian Earth Sci.* 34, 418–436. doi:10.1016/j.jseas.2008.07.003
- Yun, J., Jin, Z., and Xie, G. (2014). Distribution of Major Hydrocarbon Source Rocks in the Lower Palaeozoic, Tarim Basin. *Oil Gas Geol.* 35, 827–838. (in Chinese with English abstract). doi:10.11743/ogg201406010
- Zhang, J., Fan, T., Algeo, T. J., Li, Y., and Zhang, J. (2016). Paleo-marine Environments of the Early Cambrian Yangtze Platform. *Palaeogeogr. Palaeoclimatol. Palaeoecol.* 443, 66–79. doi:10.1016/j.palaeo.2015.11.029
- Zhang, K., Jiang, S., Zhao, R., Wang, P. F., Jia, C. Z., and Song, Y. (2022). Connectivity of Organic Matter Pores in the Lower Silurian Longmaxi Formation Shale, Sichuan Basin, Southern China: Analyses from Helium Ion Microscope and Focused Ion Beam Scanning Electron Microscope. *Geol. J.* 2022, 1–13. doi:10.1002/gj.4387
- Zhao, J., Jin, Z., Hu, Q., Liu, K., Liu, G., Gao, B., et al. (2019). Geological Controls on the Accumulation of Shale Gas: a Case Study of the Early Cambrian Shale in the Upper Yangtze Area. *Mar. Pet. Geology*. 107, 423–437. doi:10.1016/j.marpetgeo.2019.05.014
- Zheng, Y., Anderson, R. F., van Geen, A., and Kuwabara, J. (2000). Authigenic Molybdenum Formation in marine Sediments: a Link to Pore Water Sulfide in the Santa Barbara Basin. *Geochimica et Cosmochimica Acta* 64, 4165–4178. doi:10.1016/s0016-7037(00)00495-6
- Zhou, X., Chen, D., Qing, H., Qian, Y., and Wang, D. (2014). Submarine Silica-Rich Hydrothermal Activity during the Earliest Cambrian in the Tarim Basin, Northwest China. *Int. Geology. Rev.* 56 (15), 1906–1918. doi:10.1080/00206814.2014.968885
- Zhou, X., Chen, D., Dong, S., Zhang, Y., Guo, Z., Wei, H., et al. (2015). Diagenetic Barite Deposits in the Yurtus Formation in Tarim Basin, NW China: Implications for Barium and Sulfur Cycling in the Earliest Cambrian. *Precambrian Res.* 263, 79–87. doi:10.1016/j.precamres.2015.03.006
- Zhu, G., Chen, F., Chen, Z., Zhang, Y., Xing, X., Tao, X., et al. (2016). Discovery and Basic Characteristics of High-Quality Source Rocks Found in the Yuertusi Formation of the Cambrian in Tarim Basin, China. *J. Nat. Gas Geosci.* 1, 21–33. doi:10.1016/j.jnggs.2016.05.002
- Zhu, G., Chen, F., Wang, M., Zhang, Z., Ren, R., and Wu, L. (2018). Discovery of the Lower Cambrian High-Quality Source Rocks and Deep Oil and Gas Exploration Potential in the Tarim Basin, China. *Bulletin* 102, 2123–2151. doi:10.1306/03141817183
- Zhu, G., Zhang, Z., Zhou, X., Li, T., Han, J., and Sun, C. (2019). The Complexity, Secondary Geochemical Process, Genetic Mechanism and Distribution Prediction of Deep marine Oil and Gas in the Tarim Basin, China. *Earth-Science Rev.* 198, 102930. doi:10.1016/j.earscirev.2019.102930

Conflict of Interest: The authors declare that the research was conducted in the absence of any commercial or financial relationships that could be construed as a potential conflict of interest.

Publisher’s Note: All claims expressed in this article are solely those of the authors and do not necessarily represent those of their affiliated organizations, or those of the publisher, the editors, and the reviewers. Any product that may be evaluated in this article, or claim that may be made by its manufacturer, is not guaranteed or endorsed by the publisher.

Copyright © 2022 Wang, Chen, Shen and Li. This is an open-access article distributed under the terms of the Creative Commons Attribution License (CC BY). The use, distribution or reproduction in other forums is permitted, provided the original author(s) and the copyright owner(s) are credited and that the original publication in this journal is cited, in accordance with accepted academic practice. No use, distribution or reproduction is permitted which does not comply with these terms.